

# Nesting: Hierarchies of allosteric interactions

(binding potential/linkage/ligand binding/hemocyanin)

CHARLES H. ROBERT\*, HEINZ DECKER†, BROUGH RICHEY‡, STANLEY J. GILL\*§, AND JEFFRIES WYMAN\*

\*Department of Chemistry and Biochemistry, University of Colorado, Boulder, CO 80309; †Zoologisches Institut, Universität München, 8 München 2, Federal Republic of Germany; ‡Department of Chemistry, University of Wisconsin, Madison, WI 53706

Contributed by Jeffries Wyman, November 24, 1986

**ABSTRACT** A generalization of the allosteric model is presented that incorporates a hierarchy of conformational equilibria. Such a formulation draws upon structural organization already seen in many large macromolecular systems. The functional binding properties of the macromolecule reflect conformational equilibria at each structural level. Appropriate “nested” models are used to interpret structural features and functional aspects of two hemocyanin systems with a large number (12 and 24) of binding sites.

Structures of large biological macromolecules commonly show a hierarchical organization of subunits, in which a small number of subunits form “building block” assemblies that themselves build up progressively to form the holomolecule. In proteins the subunits are often well defined as polypeptide chains. In nucleic acids the subunits could be thought of as the nucleotide residues that are base-paired at one level of structure and chained together and stacked into a helix at a higher level. Macromolecules with these characteristics often present a challenge to modeling in terms of function. It is the purpose of this paper to suggest a thermodynamic framework for considering functional aspects of such organization.

Examples of hierarchy in structural organization are found readily in the oxygen-carrying proteins of arthropods and mollusks, the hemocyanins. In certain hemocyanin molecules as many as 160 ligand-binding sites are arranged in highly repetitive structures and substructures (1). An advantage of this arrangement in terms of function may be enhancement of the total cooperativity of ligand binding, arising from the large number of interacting sites; another may be extension of the range of cooperative binding, enabling the macromolecule to operate with different cooperativities in different regions of ligand activity (2). The ligand-binding curves of such molecules are often complex (2–9) and cannot be readily explained by simple models of allosteric interaction.

The hierarchy of structure apparent in these large macromolecules suggests a corresponding hierarchy of allosteric interaction and control. Such an interaction pattern has been termed “nesting” (10). In the concept of nesting, the repeated subunits or assemblies of subunits are each hypothesized to be allosteric entities. Further, they can interact by means of changes in conformation of the higher-level assembly. Thus, these units are “nested” in a given conformational environment that is a property of the higher-level structure.

In this paper we outline a general mathematical formulation of nesting models and illustrate the effects of nesting by two examples: (i) oxygen binding to tarantula hemocyanin, a 24-site macromolecule composed of repeated dodecameric assemblies, and (ii) oxygen and carbon monoxide binding to lobster hemocyanin, a dodecameric protein made up of two identical hexamers.

## STATEMENT OF THE MODEL

Nesting arises from the influence of the conformation of a given structure on the functional properties of its substructures. Thus, a nesting model can in principle become quite complex, since a substructure of a macromolecule may itself be a complicated structure, with substructures of its own. This hierarchy could be extended either upward toward larger structures or downward toward smaller ones, conformational equilibria at each structural level exerting functional influence on the properties of the next level. On the other hand, a nesting model can as well consist of a single level of influence. In this context, the popular allosteric models, the Koshland–Nemethy–Filmer (KNF; ref. 11) and the Monod–Wyman–Changeux (MWC; ref. 12), exemplify a single level of nesting (13)—that is, the subunits of a macromolecule are hypothesized in those models to bind ligand in a noncooperative manner with the binding affinity determined by the conformation of the macromolecule. Two levels of nesting are then exemplified when one hypothesizes that a large, multiple-conformation macromolecule is composed of a number of allosteric units, each with properties sensitive to the overall macromolecular conformation.

At a given level, the influence of conformation on the functional properties of the substructures may be expected to have a characteristic mechanism. For instance, on a large scale conformational change in a protein might alter  $\alpha$ -helix packing, whereas on a smaller scale the rupture of individual hydrogen bonds or salt bridges may be relevant. In a phenomenological way, however, the hierarchy of influence is self-similar—i.e., the effect can be described in the same general terms at each level. For our purposes, the degree of self-similarity in a specific macromolecular system, evident from the extent of structural hierarchy present, determines the number of levels of nesting.

We emphasize that nesting is a generalization of the original allosteric model. At a given structural level, the allosteric interactions could be modeled according to any appropriate formalism—for instance, the MWC or the KNF model. Applications making use of both of those models have appeared (2, 8). In particular, models using KNF or Pauling-type subunit interaction schemes nested inside a higher-level MWC formulation have been called “cooperon” models (14) and have been invoked in an explanation (15) of the detailed cooperative free-energy levels observed by Smith and Ackers (16) for human hemoglobin.

## THEORY

The nesting idea for a nondissociating macromolecule can be conveniently expressed in terms of the binding polynomial (17, 18), although the assumption of mass-law binding implicit in writing a binding polynomial is not required for nesting in general. The binding polynomial is similar to the grand

The publication costs of this article were defrayed in part by page charge payment. This article must therefore be hereby marked “advertisement” in accordance with 18 U.S.C. §1734 solely to indicate this fact.

Abbreviations: KNF, Koshland–Nemethy–Filmer; MWC, Monod–Wyman–Changeux.

§To whom reprint requests should be addressed.

partition function; here the free-energy states of the macromolecule, relative to its free energy in an unligated state, are defined by the number of bound ligands as well as by the conformation. In this section we first obtain the binding polynomial that applies to a macromolecule exhibiting a single level of nesting; such a formulation includes the MWC and KNF types of models. We then proceed to obtain the binding polynomial for a macromolecule with two levels of nesting interactions. The consequences of adding a second level will be demonstrated in *Applications*. In the following development we shall limit ourselves mainly to homotropic ligand linkage, although the extension to heterotropic linkage (more than one type of ligand) will be shown in one of the examples.

A direct formulation of the binding polynomial is obtained by making use of the binding potential (19).<sup>†</sup> For any nondissociating assembly, be it a multisite macromolecule or a single binding site, the binding potential  $\mathbb{J}$  and the binding polynomial  $P$  are related by

$$\mathbb{J}/RT = \ln P, \quad [1]$$

where the degree of the binding polynomial is equal to the number of binding sites in the structure. For example, a single-site binding polynomial can be written  $P = 1 + \kappa x$ , where  $x$  is the activity of ligand X and  $\kappa$  is the intrinsic site affinity for X. The specification of the binding potentials for the "building blocks" permits the construction of the binding potential of the whole macromolecule, as shown in the following sections.

**A Single Nesting Level.** The simple allosteric models are based on a single level of nesting, in which it is postulated that the macromolecule can exist in any of a number of conformations, each conformation dictating the binding properties of the subunits, and that the subunits are independent within a conformation. The binding potential of the macromolecule constrained to a conformation  $i$  is then the sum of the potentials of the subunits, each for simplicity assumed here to be a single site, in that conformation. For  $n$  subunits indexed by  $q$ ,

$$\mathbb{J}_i = \sum_{q=1}^n \mathbb{J}_{i,q}. \quad [2]$$

The binding potential for the macromolecule in equilibrium, with  $r$  conformations available to it, is then (20)

$$\text{Single level: } \mathbb{J}/RT = \ln \sum_{i=1}^r v_i^0 \exp \mathbb{J}_i/RT, \quad [3]$$

where  $v_i^0$  is the mole fraction of macromolecules in conformation  $i$  at some reference state, here specified as when the primary ligand of interest is not present.

To cast these concepts into a more practical form we utilize the relation of the binding potential to the binding polynomial, Eq. 1. The binding potentials in Eqs. 2 and 3 can be expressed in terms of appropriate binding polynomials using Eq. 1. In particular, the binding polynomial for the macromolecule with a single level of nesting is

$$\text{Single level: } P = \sum_{i=1}^r v_i^0 P_i = \sum_{i=1}^r v_i^0 \prod_{q=1}^n (1 + \kappa_{i,q} x), \quad [4]$$

where the sensitivity of the subunit  $q$  to its conformational

environment  $i$  is manifest in its affinity constant  $\kappa_{i,q}$ .<sup>‡</sup> The binding polynomial for the familiar MWC concerted two-state ( $r = 2$ ;  $i = 1$  for the "R" state and  $i = 2$  for the "T" state) model obtains when all subunits  $q$  of a conformation  $i$  are assumed equivalent with respect to ligand affinity, allowing the product in Eq. 4 to be simplified to  $(1 + \kappa_i x)^n$ . A KNF approach would specify that each conformation is defined by a given number of bound ligands, which requires that only certain terms in the expansion of the product in Eq. 4 are considered. The details of such a procedure have been examined (13).

**Two Levels of Nesting.** Now we consider an assembly of structures, each with a single level of nesting as just described. The entire assembly can exist in any of  $r'$  overall conformations, indexed by  $i'$ . The result is a sort of "super" macromolecule with two levels of allosteric interaction. In a given super conformation  $i'$  the composite single-level-nested structures are independent of one another. The binding potential of the macromolecule constrained in that overall conformation thus follows a summation over the  $n'$  allosteric structures analogous to the summation over subunits in Eq. 2:

$$\mathbb{J}_{i'}/RT = \sum_{q'=1}^{n'} \mathbb{J}_{i',q'}/RT. \quad [5]$$

Each single-level-nested structure  $q'$  of the macromolecule in a given overall conformation  $i'$  is not a single site but is an allosteric assembly with  $n$  sites. Therefore, the total number of sites in the macromolecule is  $n \cdot n'$ . Expressions of the form seen in Eqs. 2 and 3 are applicable to each structure  $q'$  as well:

$$\mathbb{J}_{i',q'}/RT = \ln \sum_{i=1}^r v_{i',q',i}^0 \exp \mathbb{J}_{i',q',i}/RT. \quad [6]$$

Similar to Eq. 3,  $v_{i',q',i}^0$  indicates the mole fraction of unligated allosteric unit  $q'$  in conformation  $i$ , under the influence of the macromolecular conformation  $i'$ .

The binding potential for the entire macromolecule at equilibrium can be expressed following Eq. 3 as

$$\text{Two levels: } \mathbb{J}/RT = \sum_{i'=1}^{r'} v_{i'}^0 \exp \mathbb{J}_{i'}/RT, \quad [7]$$

where  $v_{i'}^0$  denotes the mole fraction of the macromolecule in overall conformation  $i'$  when no ligand is present.

The binding polynomial for the entire macromolecule can then be obtained by using again Eq. 1.

Two levels:  $P =$

$$\sum_{i'=1}^{r'} v_{i'}^0 \left( \prod_{q'=1}^{n'} \left\{ \sum_{i=1}^r v_{i',q',i}^0 \left[ \prod_{q=1}^n (1 + \kappa_{i',q',i,q} x) \right] \right\} \right). \quad [8]$$

This is the general result for a macromolecule exhibiting two levels of allosteric interaction.

**MWC Modeling at Each Nesting Level.** The procedures

<sup>†</sup>The binding potential has the property  $\bar{X} = \partial \mathbb{J} / \partial \mu_x$ , where  $\bar{X}$  is the amount of ligand X present in the system relative to a reference component. If the reference component is identified as the macromolecule, then  $\bar{X}$  becomes the amount of ligand "bound" to the macromolecule in the most general sense.

<sup>‡</sup>If there is only one macromolecular conformation ( $r = 1$ ), the macromolecule behaves as a collection of independent sites. Identical site behavior of a macromolecule with respect to one type of ligand is often taken to indicate only one stable conformation of the native macromolecule. However, other conformations may be revealed through the linkage to a second ligand. In such a case the subunit affinity for the primary ligand would not depend on the macromolecular conformation but the affinity for the second ligand would vary with conformation.

employed above are appropriate for the construction of the binding potential and hence the binding polynomial applying to a macromolecule exhibiting any number of nested levels of allosteric interaction. However, it is seen that in general each additional level greatly increases the number of parameters to be determined by experiment. Practically, in the construction of a useful model only the minimum degree of nesting and the minimal allosteric description at each level are warranted. In this section we will apply a MWC model at each of two levels of nesting interaction.

A two-state MWC approximation for interaction at each level specifies  $r = 2$  and  $r' = 2$  in Eq. 8. The designations R and T will be used in keeping with the conventional MWC notation for the overall conformations  $i' = 1$  and  $i' = 2$ , and  $r$  and  $t$  are used for the conformations  $i = 1$  and  $i = 2$  of the  $n'$  identical allosteric structures comprising the macromolecule. It can be seen that there are four possible subunit environments (thus affinity states), which we shall denote R<sub>r</sub>, R<sub>t</sub>, T<sub>r</sub>, and T<sub>t</sub>. With these considerations the binding polynomial of Eq. 8 becomes

$$P = \frac{1}{1+L} \left[ \frac{1}{1+l_R}(1 + \kappa_{Rr}x)^n + \frac{l_R}{1+l_R}(1 + \kappa_{Rt}x)^n \right]^{n'} + \frac{L}{1+L} \left[ \frac{1}{1+l_T}(1 + \kappa_{Tr}x)^n + \frac{l_T}{1+l_T}(1 + \kappa_{Tt}x)^n \right]^{n'} \quad [9]$$

Here the  $v_i^j$  are given using the uppercase letter  $L$ , or  $1/(1+L)$  and  $L/(1+L)$ , where  $L$  is the equilibrium constant for the overall reaction  $R \rightarrow T$ . For the lower-level structures the  $v_i^j$  are replaced making use of the lowercase letters  $l_R$  and  $l_T$ .  $l_R$  is the equilibrium constant for the reaction  $r \rightarrow t$  of a structure nested in the R overall conformational state of the macromolecule and  $l_T$  is the constant for the  $r \rightarrow t$  equilibrium of a nested structure when the overall macromolecule is in conformational state T. All conformational equilibria are defined as applying in the absence of ligand.

In the first application presented below, that of oxygen binding to tarantula hemocyanin, the hemocyanin molecule has a structure described by a dimer of dodecamers, allowing the identification  $n' = 2$  and  $n = 12$ . A schematic representation of the relevant conformational equilibria at each structural level in this model is shown in Fig. 1 *Left*.

The lobster hemocyanin examined in the second example appears from electron micrographs to be constructed as a dimer of hexamers, or  $n' = 2$  and  $n = 6$ . Fig. 1 *Right* shows a representation of this model. Additionally, the second exam-

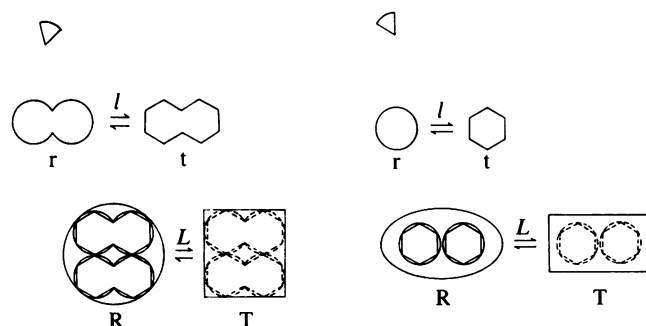


FIG. 1. Schematic representations of the 24-site tarantula hemocyanin (*Left*) and the 12-site lobster hemocyanin (*Right*). According to the nesting model, no allosteric properties are observed in an individual binding site (top). However, an assembly of such sites (middle) with two alternative conformations,  $r$  and  $t$ , shows allosteric properties or a single level of nesting. Two levels of nesting result (bottom) if a macromolecule is composed of such allosteric structures (whose equilibria are here indicated by overlapping symbols) and is itself in conformational equilibrium between two states R and T.

ple involves two competitive ligands (oxygen and CO) binding to the macromolecule at the same site, a case known as identical linkage (17), so that an additional term must be added to the individual site binding polynomials (inside the inner parentheses of Eq. 9). For example, using  $x$  for oxygen activity and  $y$  for CO activity, the R<sub>r</sub> environment for a subunit gives

$$P_{Rr} = 1 + \kappa_{Rr}^O x + \kappa_{Rr}^{CO} y. \quad [10]$$

Similar expressions apply to the R<sub>t</sub>, T<sub>r</sub>, and T<sub>t</sub> conformational environments.

## APPLICATIONS

In these examples the saturation of the macromolecule with a single ligand (moles of ligand per mole of macromolecule) is obtained from (21)

$$\bar{X} = \left( \frac{\partial \ln P}{\partial \ln x} \right)_y \quad \text{or} \quad \bar{Y} = \left( \frac{\partial \ln P}{\partial \ln y} \right)_x. \quad [11]$$

In the case of the competition experiments, where both ligands are present, the activity of the second ligand at all points of the experiment must be known and inserted into Eq. 11.

**Oxygen Binding to Tarantula Hemocyanin.** We have used a nesting model to describe oxygen binding to the hemocyanin of the tarantula *Eurypelma californicum*. A preliminary account has been published elsewhere (2). Previous analyses of oxygen equilibria with this molecule (9) demonstrated that the simple two-state MWC model is not appropriate for describing the binding curve. The molecule is composed of two identical dodecamers, each composed of seven different types of subunits. Although the electron microscopy of the intact 24-mer shows four hexameric structures, immunological and electron microscopic studies of assembly intermediates reveal that these hexamers are not formed independently but are assembled directly into dodecamers from a shared dimeric "linker" subunit between hexameric halves (22). Thus, the likely functional hierarchy of the native molecule is a dimer of dodecamers, as seen schematically in Fig. 1 *Left*.

Oxygen-binding data were obtained (2) for purified tarantula hemocyanin under conditions given in the legend of Fig. 2. The binding curve [fractional saturation ( $\theta$ ) vs. logarithm of oxygen activity relative to 1 torr (1 torr = 133 Pa)] for the native 24-site hemocyanin molecule is shown in Fig. 2 *Left*. Errors on the fractional saturation are approximately equally distributed throughout the range of saturations represented and are about one-half the height of the boxes drawn. The solid line shown in Fig. 2 is drawn from the best least-squares fit of Eq. 9 (2), and the best-fit values of the parameters are given in the legend of Fig. 2. The marked asymmetry of this curve, with high cooperativity at higher oxygen saturations, presumably reflects the physiological transport requirements of the spider.

The overall binding curve lies everywhere between two "sub"-binding curves, which are cooperative due to the presence of the additional level of allosteric interaction. For a model exhibiting only a single nesting level, like the MWC or KNF model, the overall binding curve would lie between noncooperative subbinding curves or anticooperative ones due to site heterogeneity in a given conformation. In the present example the subbinding curves of the allosteric substructures (dodecamers) are shown as dashed lines in Fig. 2. The cooperative nature of these underlying curves can be seen in this plot. A Hill plot of the data is shown in Fig. 2 *Right* along with error bars propagated through the transformation. In a macromolecule exhibiting only a single level of nesting, the subbinding curves would transform to straight

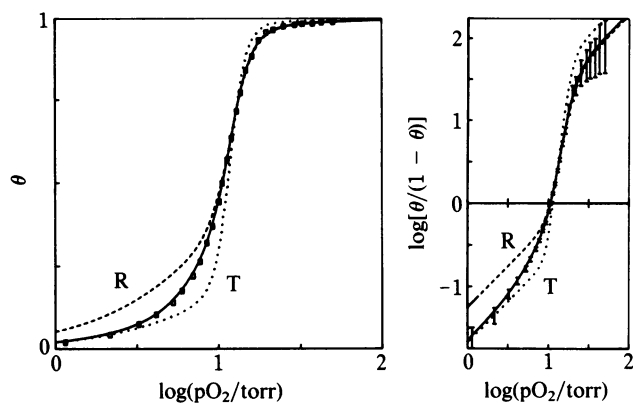


FIG. 2. (Left) Oxygen-binding curves of tarantula (*E. californicum*) hemocyanin in 0.1 M Tris, pH 8.0/1 mM MgCl<sub>2</sub>/4 mM CaCl<sub>2</sub>, 25°C (2). Boxes about data points are drawn two times the standard error of a point. The solid line is the best fit of the nesting model pictured schematically at the lower left of Fig. 1 with *R*-state parameters  $\kappa_{Rr} = 2.0 \text{ torr}^{-1}$ ,  $\kappa_{Rt} = 0.056 \text{ torr}^{-1}$ , and  $l_R = 1.6 \times 10^{14}$ ; *T*-state parameters are  $\kappa_{Tr} = 3.6 \text{ torr}^{-1}$ ,  $\kappa_{Tt} = 0.021 \text{ torr}^{-1}$ , and  $l_T = 4 \times 10^{18}$ ; overall  $L = 80$ . Errors in parameter estimates are less than half in the last place reported. Dashed and dotted lines show the underlying "subbinding curves" corresponding to the allosteric equilibria of a macromolecule hypothetically fixed in a given macromolecular form R or T, respectively. (Right) Hill plot of the binding data. The standard error of a point in the binding curve representation has been propagated through the Hill transformation in drawing error bars.

lines on the Hill plot. The cooperativity of the subbinding curves here is more obvious than in the fractional saturation plot. The macromolecule has taken a path in going from the overall T states to the overall R states that enables it to behave cooperatively in an extended range of ligand activity: low but definite cooperativity at low activities and much higher cooperativity above the half-saturation activity.

**Oxygen and Carbon Monoxide Binding to Lobster Hemocyanin.** In the case of the hemocyanin from the common lobster *Homarus americanus* the MWC model provides a good description of oxygen-binding data alone (23). However, a more extensive test by Richey *et al.* (7) of the MWC model for this molecule shows that the simple model is not appropriate. In particular, a comparison of the unligated allosteric

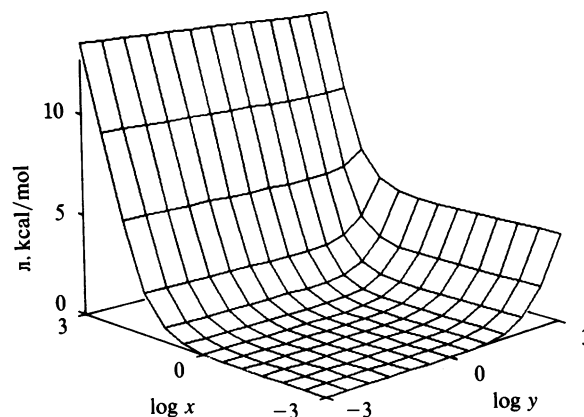


FIG. 4. Binding potential ( $J_l$ ) surface for the hemocyanin of the lobster *H. americanus* as a function of the logarithm of the activity for two competitive ligands, oxygen and carbon monoxide. The standard state activity for both gases is 1 torr.

equilibrium constant  $L$  recovered from O<sub>2</sub>- and CO-binding studies showed that a different value of this parameter was obtained with each ligand. Such an observation contradicts the MWC definition of the parameter that is defined in the absence of ligand and thus should be independent of the ligand employed. In the study of Richey *et al.*, a three-state MWC model was invoked to adequately explain all of the data. In that model, the hexamers composing the dodecameric molecule were considered to be functionally independent. Here we show that a nesting model can explain the same data while taking into account the dodecameric structure of the lobster hemocyanin in a straightforward way.

The *H. americanus* hemocyanin is a dodecameric assembly comprising two identical hexamers, each consisting of six oxygen- or CO-binding sites. The dodecamer can be reversibly dissociated into hexamers through adjustment of the calcium ion activity (24). The monomeric dissociation products (also obtained by a reversible process) exhibit homogeneous binding behavior (7).

The binding experiments of Richey *et al.* were performed with the Gill thin layer cell (25) and a modified version of the cell for fluorescence studies (26). With this technique one is

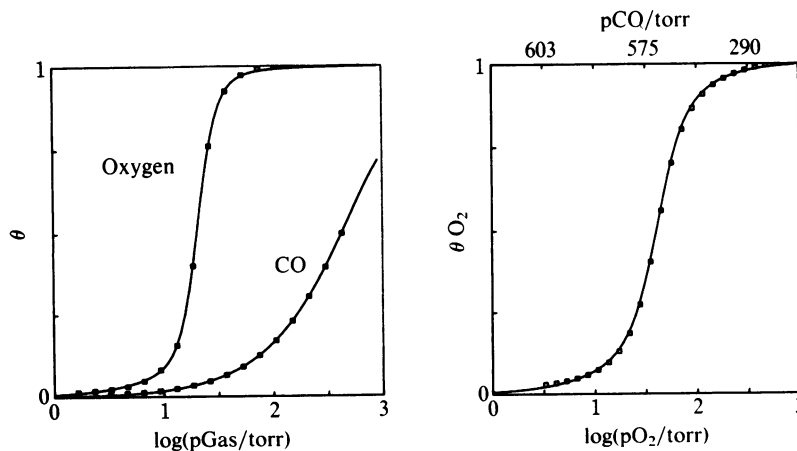


FIG. 3. Oxygen- and CO-binding curves and replacement experiment for lobster (*H. americanus*) hemocyanin [0.1 M Tris, pH 8.0/20 mM CaCl<sub>2</sub>, 25°C (7)]. Individual curves (Left) were conducted by stepwise nitrogen dilutions of the individual gas. Replacement curve (Right) was conducted by stepwise dilution of oxygen gas with carbon monoxide. CO partial pressure is found at each oxygen pressure from  $p_{CO} = 606.2 \text{ torr} - p_{O_2}$ . Boxes about data points are uniformly drawn approximately twice the maximum point error. The best fit of the theory to all data sets is shown by the solid lines, with *R*-state parameters  $\kappa_{Rr}^{O_2} = 1.7 \pm 0.2 \text{ torr}^{-1}$ ,  $\kappa_{Rt}^{CO} = 0.034 \pm 0.008 \text{ torr}^{-1}$ ,  $\kappa_{Rr}^{O_2} = 0.021 \pm 0.005 \text{ torr}^{-1}$ ,  $\kappa_{Rt}^{CO} = 0.0034 \pm 0.0004 \text{ torr}^{-1}$ , and  $l_R = (1.9 \pm 0.3) \times 10^7$ ; *T*-state parameters are  $\kappa_{Tr}^{O_2} = 0.7 \pm 0.1 \text{ torr}^{-1}$ ,  $\kappa_{Tt}^{CO} = 0.011 \pm 0.002 \text{ torr}^{-1}$ ,  $\kappa_{Tr}^{O_2} = 0.007 \pm 0.002 \text{ torr}^{-1}$ ,  $\kappa_{Tt}^{CO} = 0.0019 \pm 0.0004 \text{ torr}^{-1}$ , and  $l_T = (9 \pm 1.5) \times 10^6$ ; overall  $L = 80 \pm 15$ . Ratios of O<sub>2</sub> affinity to CO affinity are: Rr, 50; Rt, 6.2; Tr, 64; Tt, 3.7.

able to work with gaseous ligands for which there are no electrodes for determining activity—e.g., carbon monoxide. In the present study the three types of experiments from Richey *et al.* were examined: the individual oxygen- and carbon monoxide-binding curves and the replacement experiment in which oxygen replaces carbon monoxide. In all experiments the aggregation state of the macromolecule was the dodecamer (7). In the nesting model applied to the data, two MWC hexameric units ( $n = 6$ ) are nested inside a higher-level (dodecamer) assembly ( $n' = 2$ ), which can occupy either of two alternative conformations (R and T). The denotation of the subunit affinity states is the same here as in the case of the tarantula molecule: Rr, Rt, Tr, and Tt. Results of the binding experiments conducted by Richey *et al.* are shown in Fig. 3, with individual binding curves on the *Left* and a replacement experiment on the *Right*. The low affinity of this molecule for CO is readily seen in these plots. The theoretical lines shown are the best fit of the nesting model determined by simultaneous fitting of all data sets (27, 28). As shown by Richey *et al.*, the simple MWC model cannot explain these data taken together. In contrast, the nesting model fits well, and the parameters are well determined judging from the approximate one standard deviation confidence intervals given in the legend of Fig. 3.

Since binding of either ligand is at the same site, changes in the ratio of oxygen- to CO-binding constants give a measure of the local distortion of the binding site on ligation. The magnitude of this difference increases >10-fold upon conversion of the molecule from the unligated (primarily Tt) to the ligated (primarily Rr) form. A similar result was found in the study of Richey *et al.*, and this type of information appears to be relatively model independent. The effect is greater for oxygen than for CO and may indicate customization of the binding geometry for oxygen, a ligand that bridges the dinuclear coppers.

The effect of a second ligand binding to a macromolecule adds an additional dimension to the macromolecular potential surface under investigation, providing the means for more critical testing of a given model. A three-dimensional representation of the binding potential surface is shown in Fig. 4, where the two individual ligand-binding curves correspond to derivatives of cuts through the surface at fixed X (oxygen) or Y (carbon monoxide) activities. The replacement experiment corresponds to a more meandering path on the surface where both X and Y activities change.

In summary, the simple allosteric models have often proven inappropriate in dealing with the complexities of large macromolecules. We have shown that the hierarchies of structure present in these macromolecules can be used for guidance in constructing functional models. The generalization of the allosteric scheme to include more than one level of interaction, in a nested fashion, provides a rationale for interpretation of complex binding and linkage processes.

This work was supported by National Institutes of Health Grant HL22325 (S.J.G.) and National Science Foundation Grant PCM 772062 (J.W.).

1. Van Holde, K. E. & Van Bruggen, E. F. J. (1971) in *Subunits in Biological Systems*, eds. Timasheff, S. N. & Fashman, G. D. (Dekker, New York), pp. 1–53.
2. Decker, H., Robert, C. H. & Gill, S. J. (1986) in *Invertebrate Oxygen Carriers Symposium Proceedings*, ed. Linzen, B. (Springer, Berlin), pp. 383–388.
3. Miller, K. I. & Van Holde, K. E. (1974) *Biochemistry* **13**, 1668–1674.
4. Brouwer, M., Bonaventura, C. & Bonaventura, J. (1978) *Biochemistry* **17**, 2148–2154.
5. Arisaka, F. & Van Holde, K. E. (1979) *J. Mol. Biol.* **134**, 41–73.
6. Imai, K. & Yoshikawa, S. (1985) *Eur. J. Biochem.* **147**, 453–463.
7. Richey, B., Decker, H. & Gill, S. J. (1985) *Biochemistry* **24**, 109–117.
8. Coletta, M., Brunori, M. & Di Cera, E. (1986) in *Invertebrate Oxygen Carriers Symposium Proceedings*, ed. Linzen, B. (Springer, Berlin), pp. 375–381.
9. Decker, H., Savel, A., Linzen, B. & Van Holde, K. E. (1983) in *Life Chemistry Reports Supplement 1: Structure and Function in Invertebrate Respiratory Proteins*, ed. Wood, E. J. (Harwood Academic, Chur, Switzerland), pp. 251–256.
10. Wyman, J. (1984) *Quart. Rev. Biophys.* **17**, 453–488.
11. Koshland, D. E., Jr., Nemethy, G. & Filmer, D. (1966) *Biochemistry* **5**, 365–385.
12. Monod, J., Wyman, J. & Changeux, J. P. (1965) *J. Mol. Biol.* **12**, 88–112.
13. Wyman, J. (1972) *Curr. Top. Cell. Regul.* **6**, 207–223.
14. Di Cera, E. (1985) Dissertation (Universita Cattolica S.C., Rome, Italy).
15. Gill, S. J., Robert, C. H., Coletta, M., Di Cera, E. & Brunori, M. (1986) *Biophys. J.* **50**, 747–752.
16. Smith, F. R. & Ackers, G. K. (1985) *Proc. Natl. Acad. Sci. USA* **82**, 5347–5351.
17. Wyman, J. (1948) *Adv. Prot. Chem.* **4**, 407–531.
18. Schellman, J. A. (1975) *Biopolymers* **14**, 999–1018.
19. Wyman, J. (1965) *J. Mol. Biol.* **11**, 631–644.
20. Wyman, J. (1967) *J. Am. Chem. Soc.* **89**, 2202–2218.
21. Wyman, J. (1964) *Adv. Prot. Chem.* **19**, 223–286.
22. Markl, J., Decker, H., Linzen, B., Schutter, W. G., & Van Bruggen, E. F. J. (1982) *Hoppe-Seyler's Z. Physiol. Chem.* **363**, 73–87.
23. Parody-Morreale, A., Robert, C. H., Bishop, G. & Gill, S. J. (1986) in *Invertebrate Oxygen Carriers Symposium Proceedings*, ed. Linzen, B. (Springer, Berlin), pp. 389–393.
24. Morimoto, K. & Kegeles, G. (1971) *Arch. Biochem. Biophys.* **142**, 247–257.
25. Dolman, D. & Gill, S. J. (1978) *Anal. Biochem.* **87**, 127–134.
26. Decker, H., Richey, B., Lawson, R. C. & Gill, S. J. (1983) *Anal. Biochem.* **135**, 363–368.
27. Bevington, P. R. (1986) *Data Analysis and Data Reduction in the Physical Sciences* (McGraw Hill, New York).
28. Magar, M. E. (1972) *Data Analysis in Biochemistry and Biophysics* (Academic, New York).